

# High-Performance Single Fundamental Mode AlGaAs VCSELs with Mode-Selective Mirror Reflectivities

Andrea Kroner

*We present inverted surface relief vertical-cavity surface-emitting lasers (VCSELs) showing a side-mode suppression ratio above 30 dB up to maximum optical output powers of 6.3 mW and differential quantum efficiencies exceeding 90 %. An evaluation of 160 relief devices on a sample incorporating graded layers yields 157 lasers with single-mode output powers of at least 2.9 mW, proving the high effectiveness of the technique despite the comparatively simple manufacture.*

## 1. Introduction

Oxide-confined VCSELs emitting multiple transverse modes are commonly employed for short-distance data transmission. However, with the emergence of new applications like optical spectroscopy or optical sensing, there is an increasing demand for transverse single-mode VCSELs [1]. In standard devices, single-mode emission can only be achieved for small oxide apertures, involving limited maximum output power, increased ohmic resistance and reduced lifetime. More advantageous alternatives to enhance single-mode operation have been demonstrated, like long monolithic cavity VCSELs [2], antiresonant reflecting optical waveguide VCSELs [3] and VCSELs with a triangular holey structure [4]. The latter produced a record-high single-mode output power of 7.5 mW with 30 dB side-mode suppression ratio (SMSR), however, with multi-lobed far-field patterns.

In the so-called surface relief technique, an annular etch of the laser output facet lowers the mirror reflectivity particularly for higher order modes, which show higher optical intensities outside the device centre. The resulting differences in threshold gain then strongly favour the fundamental mode. In an advanced approach, the top Bragg mirror is terminated by an additional quarter-wave antiphase GaAs layer in order to decrease its reflectivity significantly. By removing the antiphase layer only in the centre of the output facet, the threshold gain for the fundamental mode is then selectively decreased. This so-called inverted relief technique requires a less precise etch depth control and higher modes experience additional absorption by the GaAs antiphase layer for emission wavelengths smaller than about 860 nm [2]. The main advantage compared to the above methods is the relatively low fabrication complexity. Furthermore, comparatively small degradations of threshold current, differential resistance or far-field pattern are observed. A high output power of 6.1 mW from a single inverted surface relief VCSEL with continuous single-mode operation and a SMSR above 30 dB has been reported [5]. Even a single-mode power of 6.5 mW was reported, however, the corresponding device showed no continuous

single-mode operation. Instead, a higher-order mode was lasing at about three times the threshold current before the VCSEL was single-mode again at higher currents [5]. Such an instability of the modal behavior questions the reliability of the mode-selective effect induced by the inverted surface relief. Therefore, a statistical investigation of this mode control technique appears to be appropriate.

In this article we investigate a large quantity of inverted relief VCSELs, demonstrate even higher output power and show much improved single-mode properties compared to reference devices for a wide range of relief diameters [6].

## 2. Device Layout and Fabrication

Figure 1 shows a schematic cross-section of the VCSEL structure and an optical microscope top view of a finished device. The epitaxial layers are designed for 860 nm emission wavelength and were grown by molecular beam epitaxy. The resonator is formed by 23 AlGaAs layer pairs in the p-doped top Bragg mirror and 39.5 pairs in the n-type bottom mirror. The active region consists of three GaAs quantum wells in a one-wavelength thick inner cavity and an adjacent AlAs layer is used for current confinement by selective oxidation. A centre circular opening is etched into the additional quarter-wave antiphase GaAs layer using citric acid. Exact alignment of surface relief and mesa was ensured by applying common optical lithography with a self-alignment technique [2]. Finally, a standard VCSEL process sequence was used to complete the devices, including oxidation and passivation. For current injection a backside n-contact and a p-contact ring with an aperture of  $16\ \mu\text{m}$  were deposited. Beside the relief devices also reference lasers were fabricated by etching the antiphase layer across the whole output facet.

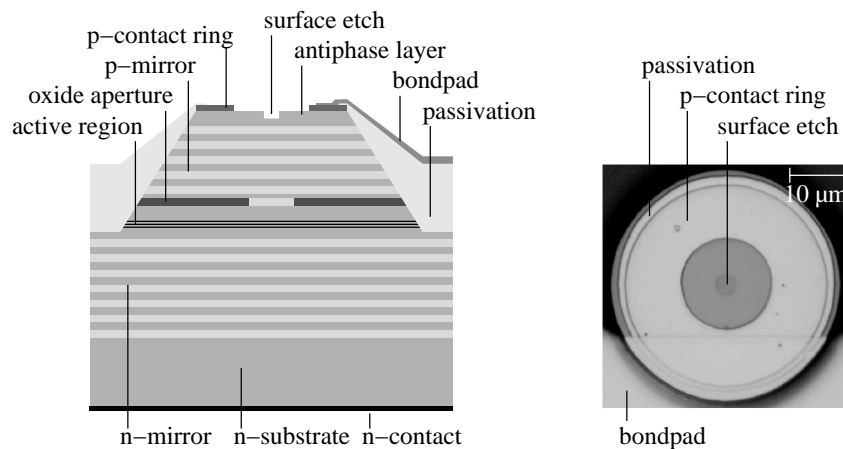


**Fig. 1:** Cross-section of the device layout (left) and optical microscope top view of a finished VCSEL (right).

### 3. Device Characterisation

Figure 2 displays the output characteristic of a reference device with an oxide aperture of about  $6\ \mu\text{m}$  and its optical spectrum at different driving currents. The laser shows a threshold current of  $0.7\ \text{mA}$ , a maximum output power of  $6.8\ \text{mW}$  (measured with an integrating sphere at room temperature) and a differential quantum efficiency of  $44\%$ . Even for small currents close to threshold, no single-mode operation with a SMSR of more than  $30\ \text{dB}$  is observed and the spectrum gets highly multimode for higher currents. Figure 3 shows the same measurements for a nearby laser on the same sample, which is nominally identical except for a surface relief with a diameter of  $3.3\ \mu\text{m}$  and an etch depth of  $58\ \text{nm}$ , as determined by atomic force microscope measurements. The relief device shows a clearly increased threshold current of  $3.1\ \text{mA}$  due to the effectively decreased mirror reflectivity. On the other hand, the differential quantum efficiency has increased to  $92\%$ , supported by the supply of carriers from the outer part of the active layers underneath the unetched region. The optical spectra confirm a SMSR exceeding  $30\ \text{dB}$  up to thermal rollover. The laser delivers a maximum single-mode output power of  $6.3\ \text{mW}$  at a driving current of  $12\ \text{mA}$ , which is to our knowledge the highest reported value for a relief VCSEL with continuous single-mode operation. Both devices have similar, low differential resistances of  $89\ \Omega$  (reference) and  $84\ \Omega$ .

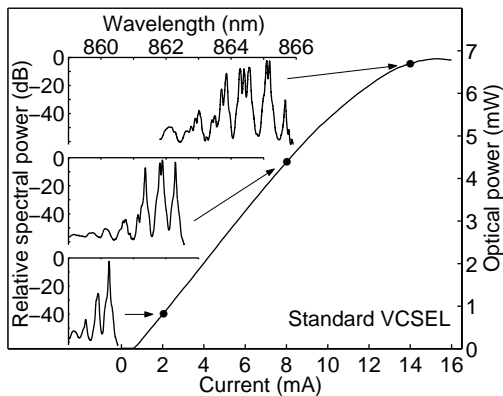


**Fig. 2:** Output characteristic of a  $6\ \mu\text{m}$  active diameter reference VCSEL without relief.

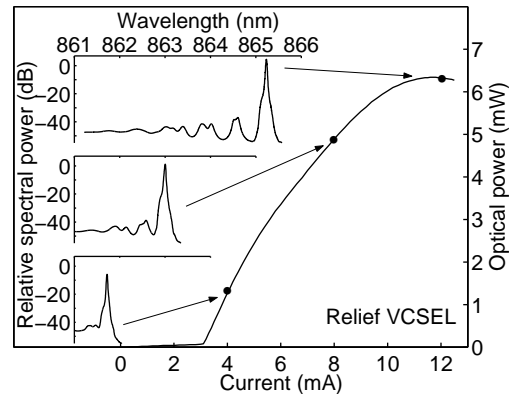


**Fig. 3:** Output characteristic of a  $6\ \mu\text{m}$  active diameter VCSEL with  $3.3\ \mu\text{m}$  relief diameter.

Figures 4 and 5 show the far-field patterns for a reference and a relief device at high currents, where both show similar output powers ( $6.6$  and  $6.3\ \text{mW}$ , respectively). The enhanced single-mode operation of the relief device results in a Gaussian-shaped beam profile and a strongly decreased full-width-at-half-maximum (FWHM) of  $7.6^\circ$  compared to  $21.3^\circ$ . Almost no side-lobes are observed.

Beside the  $6\ \mu\text{m}$  oxide apertures, also relief VCSELs with active diameters of  $4$  and  $8\ \mu\text{m}$  are contained in the investigated sample. With both aperture sizes, enhanced single-mode operation is achieved, however, the smaller devices show less output power, owing to the smaller active area. The larger devices provide similar single-mode output power as the  $6\ \mu\text{m}$  VCSELs, but show much higher threshold currents due to decreased optical guiding of the fundamental mode. Also lasing of a higher-order mode close to threshold

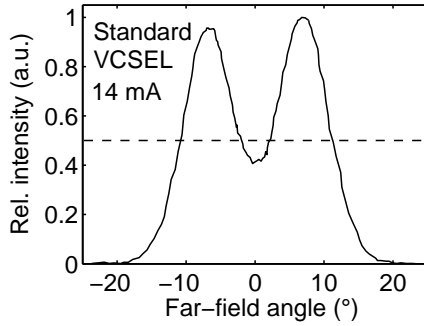


**Fig. 4:** Far-field pattern of a 6  $\mu\text{m}$  active diameter reference VCSEL without relief at 14 mA driving current.

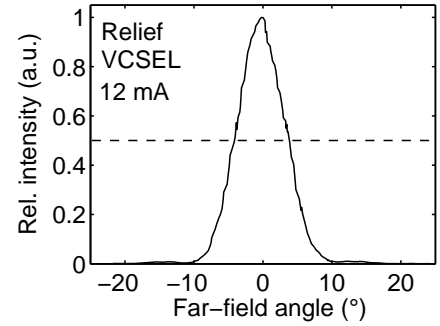


**Fig. 5:** Far-field pattern of a 6  $\mu\text{m}$  active diameter VCSEL with 3.0  $\mu\text{m}$  relief diameter at 12 mA driving current.

could be observed. Therefore we concentrated on the 6  $\mu\text{m}$  active diameter lasers for the investigations to follow.

#### 4. Statistic Investigations

To substantiate the mode-selective effect of the surface relief, a significant number of VCSELs on the same sample were characterized. The sample is subdivided into unit cells, each containing four relief devices and two reference devices, which are separated by 250  $\mu\text{m}$ . The surface reliefs have nominal diameters of 3.0, 3.2, 3.4 and 3.6  $\mu\text{m}$ . However, deviations of at least  $\pm 0.1 \mu\text{m}$  have to be taken into consideration, especially when comparing distant positions on the sample. To allow statistical conclusions, 75 reference devices and 160 relief devices from 44 unit cells were investigated. Due to a gradient in layer thicknesses, originating from the epitaxial growth process, the cavity resonance frequency varies over the sample, leading to emission wavelengths ranging from 820 to 870 nm. Since the quantum wells are optimised for 860 nm emission, lasers with short wavelengths experience less gain, resulting in lower output powers.

Figure 6 shows a schematic top view of the sample, where each rectangle represents one laser and its color indicates the maximum single-mode output power. The measurements were performed at room temperature, and a collimating objective together with a silicon photodiode were used for detection, incurring losses of about 3%. Defective devices mainly have a completely metallised output facet owing to fabrication imperfections and are not considered in the evaluation. Only one of the reference devices provides a single-mode output power of more than 1.0 mW, whereas 65% show no single-mode emission at all. On the other hand, 48% of the relief VCSELs have single-mode powers of at least 5.0 mW, 3% emit not less than 6.0 mW. Highest output power is found in the region of high gain (top right in Fig 6). A minimum single-mode output power of 2.9 mW is achieved for 98% of the relief VCSELs. The missing devices show no single-mode emission due to processing errors resulting in a too large oxide aperture.

Concerning the relief diameter, higher single-mode powers are commonly obtained for smaller reliefs, since devices with large reliefs tend to multimode emission at high currents.

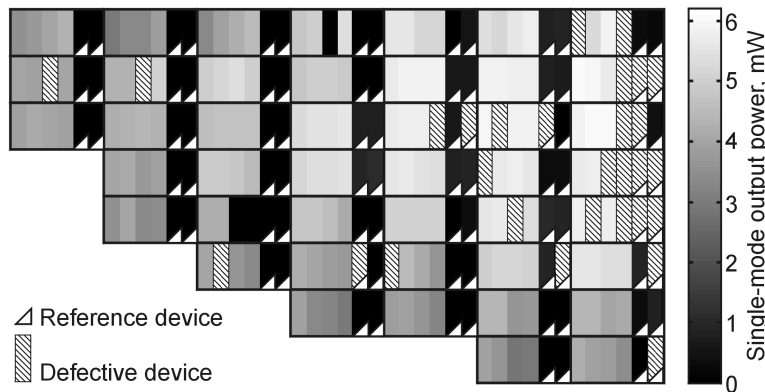


**Fig. 6:** Schematic top view of the examined sample showing the distribution of maximum single-mode output powers. Each rectangle refers to one laser.

Since the varying detuning of the sample has a much stronger influence on the device performance than the relief variations, a direct comparison of devices is only reasonable if their distance is sufficiently small. As an example, Fig 7 shows the output characteristics of four adjacent VCSELs of the same unit cell with surface reliefs of 3.6, 3.4, 3.2 and 3.0  $\mu\text{m}$  diameter. The 3.6 and 3.4  $\mu\text{m}$  devices are single-mode only up to driving currents of 10.9 and 12.3 mA, respectively, as indicated by kinks in the power curves. Therefore, their single-mode output power is limited to 5.4 and 5.5 mW, respectively. For the 3.2  $\mu\text{m}$  relief size, no higher-order mode starts to lase and a maximum single-mode output power of 5.7 mW is reached. However, at the same time, the threshold current increases by 0.6 mA, due to the reduced overlap between the fundamental mode and the surface etch. So a further reduction of the relief to 3.0  $\mu\text{m}$  eventually diminishes the output power by thermal effects.

The scaling behavior described above can be generally observed and in most cases the maximum single-mode output power within a unit cell was found for the 3.0 or 3.2  $\mu\text{m}$  relief diameter devices. Exceptions are mainly located at the upper left region of the sample, which is attributed to slightly larger oxide apertures in this area. The suitability of the smaller relief sizes is also demonstrated in the lower part of Fig 8. Here, the maximum single-mode output power of each working relief device is normalized to the single-mode output power of the nearest VCSEL with 3.6  $\mu\text{m}$  relief diameter in order to eliminate the influence of the varying resonance frequency. The figure shows the mean increase in single-mode power for devices with the same nominal relief size in dependence on the relief diameter. On average, a 4% higher output power is achieved by the VCSELs with 3.2  $\mu\text{m}$  relief diameter compared to the devices with the largest relief. In the upper part of Fig 8, the same analysis was done for the threshold current of the relief VCSELs. Here, a strong increase of the threshold with decreasing relief diameter at a rate of approximately 44%/ $\mu\text{m}$  is observed.

Although the single-mode output power is significantly increased by the inverted surface relief technique, a stable polarisation of the fundamental mode is not ensured. This is due to the fact that the relief itself is circular and no further modifications were applied to

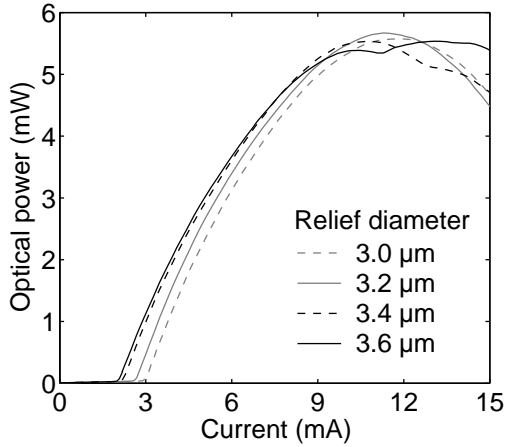


**Fig. 7:** Light output curves of four adjacent VCSELs of the same unit cell with varying surface relief diameter.

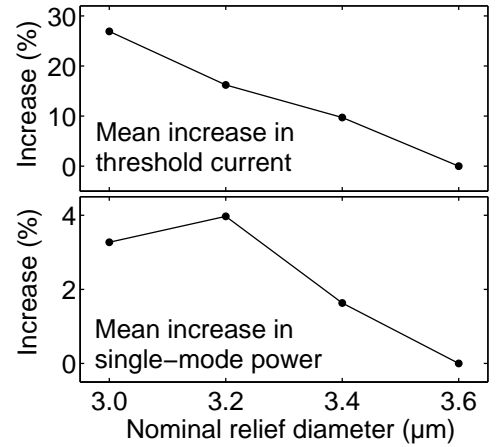


**Fig. 8:** Mean increase in threshold current (top) and single-mode output power (bottom), normalized to the devices with 3.6  $\mu\text{m}$  relief diameter.

break the rotational device symmetry. However, by combining the relief with an etched linear surface grating, reliable polarisation control is achieved in addition to enhanced single-mode output power [7, 8]. The optimum device parameters determined in this paper can therefore serve as a basis for a further increase of the single-mode output power of grating relief VCSELs.

## 5. Conclusion

We have fabricated VCSELs with an inverted surface relief using standard optical lithography and wet etching, producing devices with continuous single-mode operation of up to 6.3 mW, a SMSR above 30 dB and FWHM far-field angles below  $8^\circ$ . Reference devices show no or only weak single-mode emission. The examination of 160 relief devices on an inhomogeneous sample yielded 157 VCSELs with single-mode output powers above 2.9 mW. Among these, 76 devices delivered more than 5 mW, and best performance was generally observed for devices with 3.2  $\mu\text{m}$  relief diameter and 6  $\mu\text{m}$  oxide apertures. These results strongly confirm the suitability of the inverted surface relief technique for single-mode enhancement, since it is effective and reliable as well as relatively simple in fabrication.

## Acknowledgment

We wish to thank the German National Academic Foundation for supporting the Ph.D. thesis associated with this work and former VCSEL group member H.J. Unold for mask design.

## References

- [1] D. Wiedenmann, M. Grabherr, R. Jäger, and R. King, “High volume production of single-mode VCSELs”, in *Vertical-Cavity Surface-Emitting Lasers X*, C. Lei, K.D. Choquette (Eds.), Proc. SPIE 6132, pp. 613202-1–12, 2006.
- [2] H.J. Unold, S.W.Z. Mahmoud, R. Jäger, M. Golling, M. Kicherer, F. Mederer, M.C. Riedl, T. Knödl, M. Miller, R. Michalzik, and K.J. Ebeling, “Single-mode VCSELs”, in *Vertical-Cavity Surface-Emitting Lasers VI*, C. Lei, S.P. Kilcoyne (Eds.), Proc. SPIE 4649, pp. 218–229, 2002.
- [3] D. Zhou and L.J. Mawst, “High-power single-mode antiresonant reflecting optical waveguide-type vertical-cavity surface-emitting lasers”, *IEEE J. Quantum Electron.*, vol. 38, no. 12, pp. 1599–1606.
- [4] A. Furukawa, S. Sasaki, M. Hoshi, A. Matsuzono, K. Moritoh, and T. Baba, “High-power single-mode vertical-cavity surface-emitting lasers with triangular holey structure”, *Appl. Phys. Lett.*, vol. 85, no. 22, pp. 5161–5163, 2004.
- [5] Å. Haglund, J.S. Gustavsson, J. Vukusic, P. Modh, and A. Larsson, “Single fundamental mode output power exceeding 6 mW from VCSELs with a shallow surface relief”, *IEEE Photon. Technol. Lett.*, vol. 16, no. 2, pp. 368–370, 2004.
- [6] A. Kroner, F. Rinaldi, J.M. Ostermann, and R. Michalzik, “High-performance single fundamental mode AlGaAs VCSELs with mode-selective mirror reflectivities”, *Optics Communications*, vol. 270, no. 2, pp. 310–313, 2007.
- [7] J.M. Ostermann, P. Debernardi, C. Jalics, and R. Michalzik, *IEEE J. Select. Topics Quantum. Electron.*, vol. 11, no. 1, pp. 982–989, 2005.
- [8] J.M. Ostermann, F. Rinaldi, P. Debernardi, and R. Michalzik, “VCSELs with enhanced single-mode power and stabilized polarization for oxygen sensing”, *IEEE Photon. Technol. Lett.*, vol. 17, no. 11, pp. 2256–2258, 2005.